Available online at www.sciencedirect.com
ScienceDirect
Journal of Solid State Chemistry 179 (2006) 3324–3329
JOURNAL OF SOLID STATE CHEMISTRY
www.elsevier.com/locate/jssc

Densely packed single-crystal $Bi_2Fe_4O_9$ nanowires fabricated from a template-induced sol–gel route

Zhi Yang[a], Yi Huang[b], Bin Dong[b], Hu-Lin Li[b], San-Qiang Shi[a,*]

[a]*Department of Mechanical Engineering, The Hong Kong Polytechnic University, Hung Hom, Kowloon, Hong Kong, China*
[b]*College of Chemistry and Chemical Engineering, Lanzhou University, Lanzhou 730000, China*

Received 10 February 2006; received in revised form 10 June 2006; accepted 26 June 2006
Available online 29 June 2006

Abstract

Densely packed single-crystal $Bi_2Fe_4O_9$ nanowires were successfully synthesized by a template-induced citrate-based sol–gel process. The structural properties of the nanowires were characterized using many techniques. The results of scanning electron microscopy (SEM) and transmission electron microscopy (TEM) revealed that $Bi_2Fe_4O_9$ nanowires possessed a uniform length and diameter, which were controlled by the thickness and the pore diameter of the applied porous anodic aluminum oxide (AAO) template, respectively. The results of X-ray diffraction (XRD) and the selected area electron diffraction (SAED) indicated that $Bi_2Fe_4O_9$ nanowires had an orthorhombic single-crystal structure. Furthermore, the energy-dispersive X-ray (EDX) spectroscopy demonstrated that the stoichiometric $Bi_2Fe_4O_9$ was formed. The possible formation mechanism of nanowires was also discussed.

Keywords: $Bi_2Fe_4O_9$ nanowires; Sol–gel; Template

1. Introduction

Among various classes of nanostructures, nanowires have attracted extensive synthetic attention as a result of their novel morphology-dependent properties, which are different from that of the bulk. The potential applications of nanowires in the nanoelectronic and nanophotonic devices, sensors, catalysts, and data storages have been also proposed [1–3]. Recently, much attention has been paid to the preparation of composite oxides nanowires because of their interesting and distinctive physical and chemical properties. Several composite oxide nanowires, such as $LaFeO_3$ [4], and $LaNiO_3$ [5], have been successfully synthesized. Up to now, however, the synthesis of nanowires of multi-component oxides is still a challenging issue.

In this paper, we report the synthesis of composite oxides $Bi_2Fe_4O_9$, a well-known material that has been the subject of intensive investigations over the years [6–9]. $Bi_2Fe_4O_9$ compounds have been widely used as high-performance sensors, catalysts, and other functional materials [10–12]. Early in 1964, $Bi_2Fe_4O_9$ powders have been synthesized by the method of solid-state sintering at temperatures over 1123 K [6]. However, because of some disadvantages of this method such as high temperature, easy impurity contamination, relatively large dimension, and difficult control of synthesis conditions, new synthesis methods have been investigated until now. Recently, $Bi_2Fe_4O_9$ nanoparticles and submicron-sized cubes have been prepared by means of hydrothermal synthesis [13] and solid-state reaction [14], respectively. Xiong et al. [13] have prepared sheet-like $Bi_2Fe_4O_9$ nanoparticles at 453 K via a hydrothermal process. Park et al. [14] have employed a molten salt technique for the synthesis of submicron-sized $Bi_2Fe_4O_9$ cubes using Bi_2O_3 and Fe_2O_3 as starting materials.

Despite the evident importance of $Bi_2Fe_4O_9$ as a functional material, very few reports have associated with its nanoscale structural motifs. The fabrication of well-defined size of $Bi_2Fe_4O_9$ is of fundamental importance in investigating the size correlation of the basic physical properties of these materials, with implications for their

*Corresponding author. Fax: +852 2365 4703.
E-mail address: mmsqshi@polyu.edu.hk (S.-Q. Shi).

0022-4596/$ - see front matter © 2006 Elsevier Inc. All rights reserved.
doi:10.1016/j.jssc.2006.06.029

device applications. For future applications of nanomaterials, such as elements of devices, it is evident that determining particle shapes (e.g., nanowires) are also crucial [15]. To the best of our knowledge, no reports on the synthesis of $Bi_2Fe_4O_9$ nanowires have been published to date.

As an important way to control the size and shape of the nanomaterials, the anodic aluminum oxide (AAO) template method has attracted more and more attention in preparing ordered carbon nanotubes [16], semiconductor nanowire arrays [17,18], magnetic nanowire arrays [19], etc. AAO template is considered as a particularly attractive template for fabricating one-dimensional nanomaterials because its pore density is high, its pore distribution is uniform and its pore diameter is easily controlled [20,21]. When anodized in an acidic electrolyte, aluminum forms a porous oxide with uniform and parallel pores open at one end and sealed at the other. The channel diameter and pore density are controlled by the choice of electrolyte and by the anodizing voltage [22,23].

Sol–gel method has become a popular method for preparation of inorganic materials and has a number of advantages over many conventional synthetic procedures such as high purity, homogeneous multi-component and easy chemical doping of the materials prepared. Sol–gel synthesis via the citrate precursor route, one of sol–gel method, is well known. This method has the advantages of both wet-chemical and solid-state synthesis methods, such as low-temperature synthesis (less than 1273 K), well-dispersed nanoparticles, inexpensive precursors, and ease of preparation.

In the current work, we have combined the concepts of citrate-based sol–gel synthesis and template preparation of nanomaterials to yield a novel general route for fabricating densely packed $Bi_2Fe_4O_9$ nanowires for the first time. This was accomplished by conducting sol–gel synthesis within the pores of nanoporous templates, resulting in the formation of mono-dispersed $Bi_2Fe_4O_9$ nanowires.

2. Experimental section

2.1. Membrane preparation

High-purity aluminum foil (99.999%) employed in this experiment was ultrasonically degreased in acetone for 10 min, etched in 1.0 mol L^{-1} NaOH at room temperature for 3 min to remove the native oxide, washed thoroughly with distilled water, electropolished in a mixed solution of $HClO_4$:CH_3CH_2OH = 1:4(V/V) for 5 min to provide a smooth surface and promptly rinsed with distilled water. Afterwards, the resulted clean aluminum foil was anodized at 80 V_{dc} for 2 h in 0.5 mol L^{-1} phosphoric acid solution. Each sample was then placed into saturated $HgCl_2$ solution for 1 h to separate the template membrane from the aluminum substrate. The membrane was rinsed with distilled water and immersed in 0.5 mol L^{-1} H_3PO_4 solution for about 15 min at 328 K in order to dissolve the barrier-type part of nanoholes on the bottom. The obtained AAO template had a highly ordered porous structure with very uniform and nearly parallel pores, which could be organized in an almost precise structure. The AAO template was characterized by atomic force microscopy (AFM, Solver P47, Russia) and scanning electron microscopy (SEM) (JSM-5600LV, Japan).

2.2. Preparation of $Bi_2Fe_4O_9$ nanowires

The $Bi_2Fe_4O_9$ precursors in this work were prepared by means of sol–gel method. Analytical grade bismuth nitrate ($Bi(NO_3)_3 \cdot 5H_2O$), ferric nitrate ($Fe(NO_3)_3 \cdot 9H_2O$), citric acid ($C_6H_8O_7 \cdot H_2O$) and aqueous ammonia ($NH_3 \cdot H_2O$) were used as raw materials. 0.01 mol $Bi(NO_3)_3 \cdot 5H_2O$ and 0.01 mol $Fe(NO_3)_3 \cdot 9H_2O$ were first dissolved in 50 ml deionized water and then 0.02 mol citric acid was added to the above solution. The molar amount of citric acid was equal to total molar amount of metal nitrates in solution. Aqueous ammonia was slowly added in order to adjust the pH value of the solution in the range of 6~7 and stabilize the nitrate–citrate solution. During this procedure, the solution was kept at a temperature of 333 K and with vigorous stirring. Thus a transparent and homogeneous sol was obtained. The AAO template was immersed into this sol for 30 min and then removed. Excess sol on the template surface was wiped off using a laboratory tissue, followed by drying under vacuum at 323 K for 2 h. Subsequently, the template was put into a tube furnace. The temperature of the tube furnace was increased to 393 K and kept constantly at this temperature for 30 min. Then it was increased to 1073 K and kept for 3 h.

2.3. Characterization of $Bi_2Fe_4O_9$ nanowires

The structure and morphology properties of as-synthesized $Bi_2Fe_4O_9$ nanowires were characterized by many techniques. Prior to SEM characterization, several drops of 3 mol L^{-1} NaOH were added to the sample to dissolve the partial AAO template and Au was sputtered onto the surface of samples in order to increase their conductivity. To confirm the existence of $Bi_2Fe_4O_9$ nanowires, the concentrations of Bi and Fe elements in the $Bi_2Fe_4O_9$ nanowires were determined by the energy-dispersive X-ray (EDX) analysis using a Kevex system (USA) attached to the scanning electron microscope. Transmission electron microscopy (TEM) images and selected area electron diffraction (SAED) patterns were obtained using a Hitachi-600 microscope. It was used to observe the morphology and degree of agglomeration of the nanowires. Before TEM observation, the AAO template was dissolved by using 3 mol L^{-1} NaOH, and then diluted with distilled water for three times. Droplets of the solution containing $Bi_2Fe_4O_9$ nanowires were dropped onto the copper grids. The X-ray diffraction (XRD) patterns for $Bi_2Fe_4O_9$ nanowires were recorded with a diffractometer (Rigaku D/MAX-2400, Japan) using Cu$K\alpha$ radiation ($\lambda = 1.54184$ Å). The current

and voltage during the measurements were 60 mA and 40 kV, respectively. The scanning rate was $10^\circ\,min^{-1}$ and the 2θ scanning range was from 20° to 80°.

3. Results and discussion

3.1. Characterization of the membrane

As indicated in Fig. 1(a), the pores in the membrane are arranged in a columnar lattice cell. Perfect pore arrays can be observed, which are separated from neighboring aluminum oxide domains with a different orientation of the pore lattice by grain boundaries. Fig. 1(b) depicts the cross-section SEM image of the AAO template with pores parallel to each other and perpendicular to the surface of the membrane. Here, the pores of the membrane are about 100 nm in diameter and about 50 μm in length with a pore density of about $10^9 \sim 10^{10}\,cm^{-2}$.

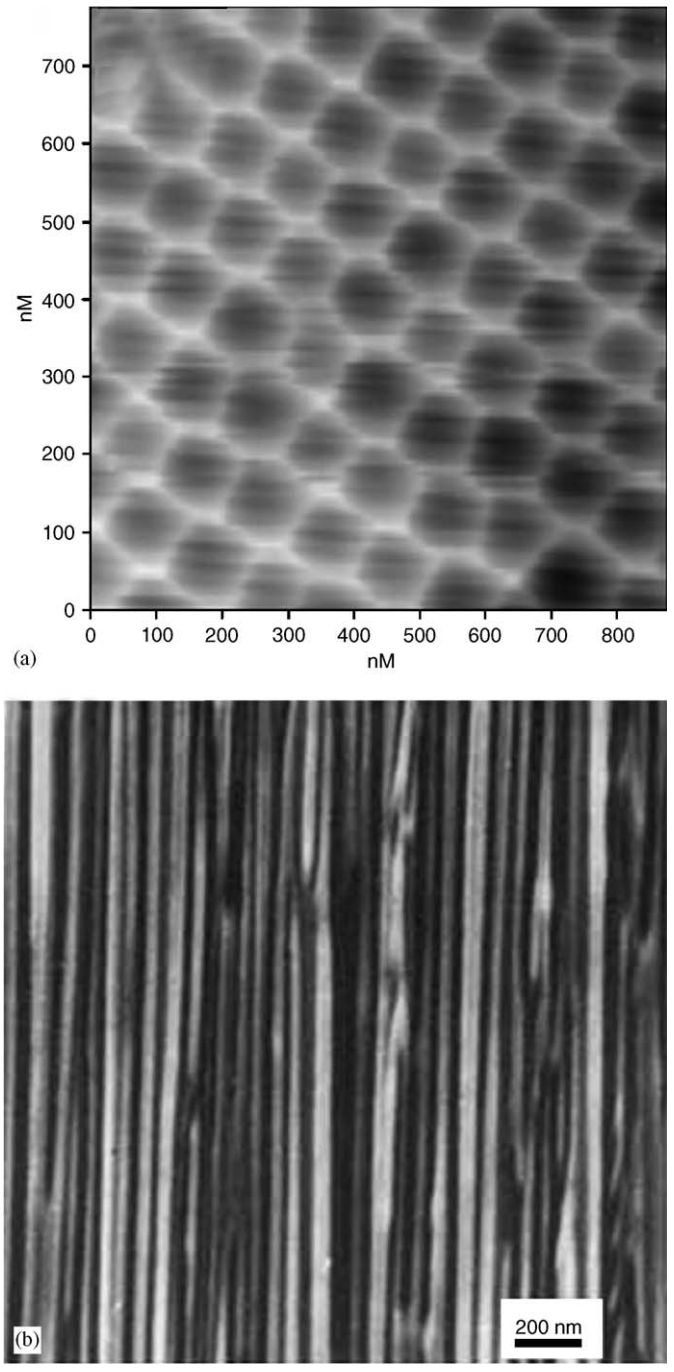

Fig. 1. (a) AFM image of the surface of AAO template under tapping mode and (b) SEM image of cross-section of AAO template.

3.2. SEM and EDX analysis of $Bi_2Fe_4O_9$ nanowires

Figs. 2(a) and 2(b) shows SEM images of $Bi_2Fe_4O_9$ nanowires grown in the AAO template. The micrographs show that the nanowires are roughly parallel to each other, vertically oriented on the AAO template to form an array. It is also found that the length of $Bi_2Fe_4O_9$ nanowires is

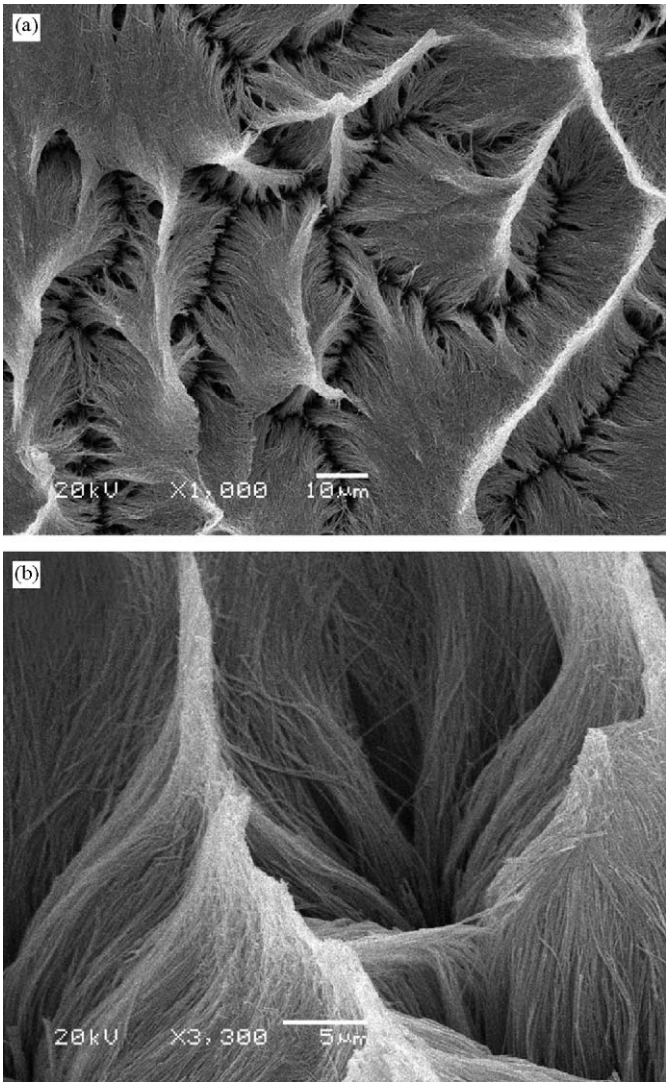

Fig. 2. SEM images of $Bi_2Fe_4O_9$ nanowires after AAO template is partly dissolved: (a) top view in low magnification and (b) cross-section in high magnification.

about 50 μm, which is corresponding to the thickness of the AAO template. The diameter of these nanowires is about 100 nm, which is equivalent to the pore diameter of the template. Fig. 2(a) shows several clusters of nanowires. The clusters were formed by removing the framework of the AAO template. When the top alumina of the AAO template is dissolved away, the nanowires embedded in the template release gradually and incline to agglomerate together. Fig. 2(a) also shows that $Bi_2Fe_4O_9$ nanowires are abundant, uniform and densely packed in a large scale. Fig. 2(b) shows an area where the alumina matrix of the AAO template has been dissolved away and large quantities of $Bi_2Fe_4O_9$ nanowires remain.

In order to confirm the chemical composition of $Bi_2Fe_4O_9$ nanowires, EDX spectroscopy are taken at a number of selected positions of the sample. As shown in Fig. 3, the sample contains Bi and Fe in addition to signals of alumina. The result shows the atomic ratio of Bi/Fe approximately equals to 1:2. The percentage concentrations of Bi and Fe in the $Bi_2Fe_4O_9$ nanowires determined by EDX agree with that obtained by stoichiometric analysis. The peak of element Au (not marked in Fig. 3) is obtained because Au is sputter-covered on the surface in order to provide conductibility.

3.3. TEM and SAED analysis of $Bi_2Fe_4O_9$ nanowires

A TEM image of $Bi_2Fe_4O_9$ nanowires is depicted in Fig. 4(a). Fig. 4(a) shows several $Bi_2Fe_4O_9$ nanowires, in which some of these nanowires cross and overlap with each other. This image also shows that the diameter of $Bi_2Fe_4O_9$ nanowires is about 100 nm, which approximately equals to that of the nanochannels of the employed AAO template. Although the lengths of nanowires in the Fig. 4(a) are much less than 50 μm, it does not imply that the as-grown nanowires are really so short. It may be attributed to the fact that the nanowires are easily broken by the ultrasonic stirring process during the preparation of samples for TEM observation. These nanowires are uniformly distributed, which indicates that the alumina matrix is dissolved completely. It can be also seen that the surfaces of these nanowires are smooth. The corresponding SAED pattern (Fig. 4(b)) taken from individual nanowire shows the presence of sharp diffraction spots indicating the formation of well-developed, single-crystal $Bi_2Fe_4O_9$. Lots of individual $Bi_2Fe_4O_9$ nanowires were examined. We note that the electron diffraction patterns obtained from different single nanowire also show similar sharp diffraction spots.

3.4. XRD analysis of $Bi_2Fe_4O_9$ nanowires

The XRD pattern of $Bi_2Fe_4O_9$ nanowires after heat treatment at 1073 K for 3 h is shown in Fig. 5(a). All the observed XRD peaks present sharp reflections, showing that the nanowires are well crystallized. In effect, all diffraction peaks in Fig. 5(a) can be indexed to the orthorhombic structure of $Bi_2Fe_4O_9$ (space group: *Pbam*) with lattice constants of $a = 7.965$ Å, $b = 8.440$ Å, and $c = 5.994$ Å, which are in good agreement with literature results (i.e., JCPDS: 25-0090, Fig. 5(b)). All of the diffraction peaks are assigned to crystalline composite oxides $Bi_2Fe_4O_9$ and no other features are observed [13,14].

3.5. The possible mechanism of the fabrication of $Bi_2Fe_4O_9$ nanowires

The EDX, SAED, and XRD data show that the $Bi_2Fe_4O_9$ nanowires are formed. Fig. 6 shows the possible

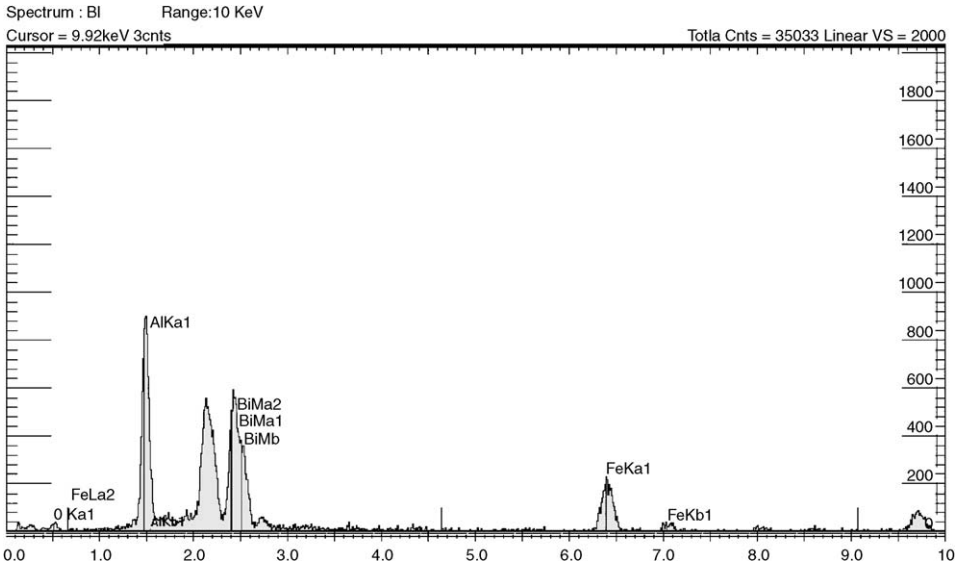

Fig. 3. EDX patterns of $Bi_2Fe_4O_9$ nanowires after AAO template is partly dissolved.

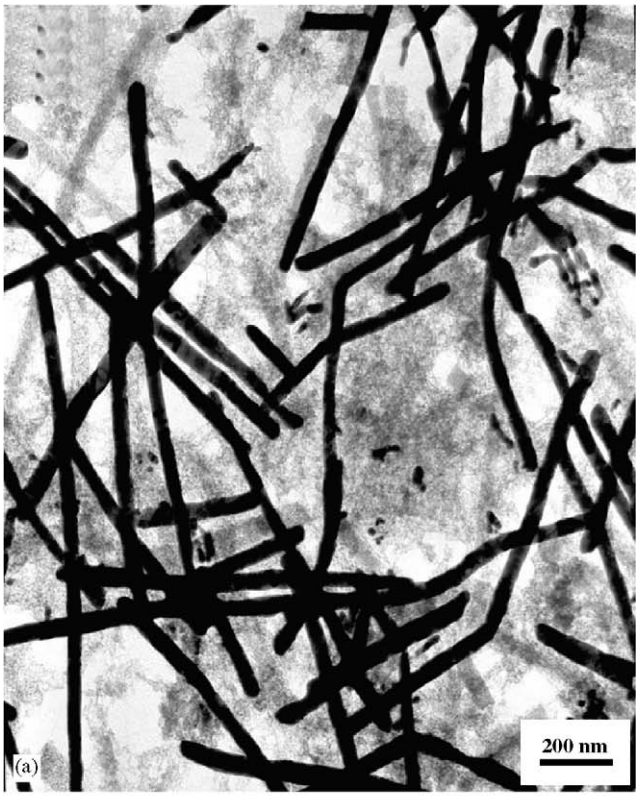

Fig. 4. (a) A TEM image of $Bi_2Fe_4O_9$ nanowires after removing AAO and (b) the corresponding selected-area electron diffraction for $Bi_2Fe_4O_9$ nanowires.

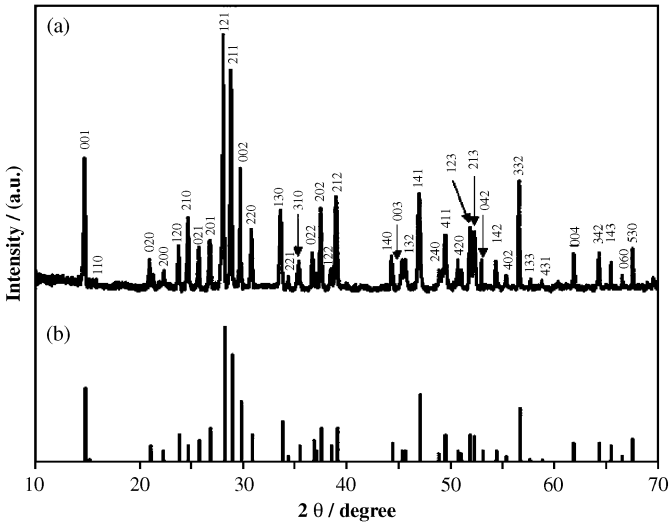

Fig. 5. XRD patterns of $Bi_2Fe_4O_9$ nanowires.

formation process of $Bi_2Fe_4O_9$ nanowires. The fact that $Bi_2Fe_4O_9$ nanowires are initially formed in AAO template indicated that the $Bi_2Fe_4O_9$ sol particles adsorb to the porewalls of template. It is well known that at the pH values (pH = 6~7) used here the sol particles are weakly positively charged. Hence, electrostatic interactions between these positively charged sol particles and anionic sites on the pore wall of AAO template result in the adsorption of sol particles inside the pores [4,5,24]. Then $Bi_2Fe_4O_9$ nanowires are formed at 1073 K. In this process, the nanochannels of the AAO template act as micro-cells in which $Bi_2Fe_4O_9$ nanowires are formed, shaped, and subsequently changed into the nanocrystalline composite oxides during heat treatment.

4. Conclusion

In conclusion, densely packed $Bi_2Fe_4O_9$ nanowires arrays have been prepared successfully by a citrate-based sol–gel method combined with porous AAO template. The single-crystal $Bi_2Fe_4O_9$ nanowires were subsequently characterized by a number of techniques, including SEM, EDX, TEM, SAED and XRD measurements. The SEM and TEM results showed that $Bi_2Fe_4O_9$ nanowires were abundant, parallel and densely packed in a large scale. XRD patterns indicated that $Bi_2Fe_4O_9$ naowires were of orthorhombic structure. The result of SAED demonstrated that $Bi_2Fe_4O_9$ nanowires were single crystals. EDX analysis demonstrated that stoichiometric $Bi_2Fe_4O_9$ nanowires were formed. This facile method of preparing densely packed $Bi_2Fe_4O_9$ nanowires at a large scale might be important for many applications in nanomaterials.

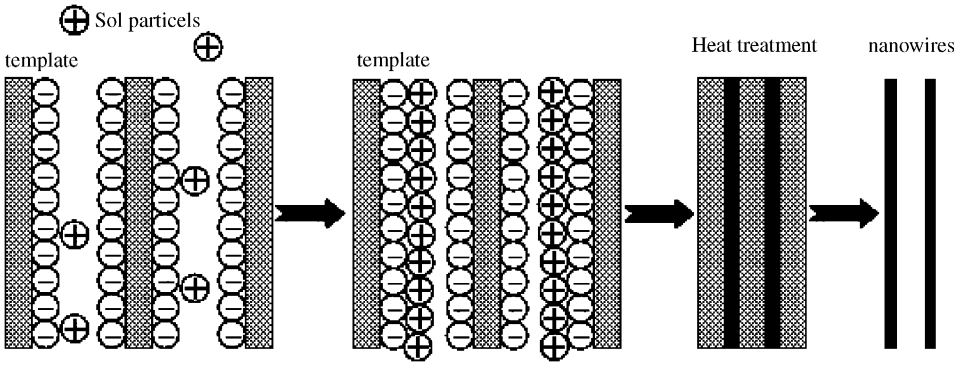

Fig. 6. A schematic diagram of the possible growth mechanism of $Bi_2Fe_4O_9$ nanowires in the AAO template.

Acknowledgment

This work was supported by a research grant from the Research Grant Council of Hong Kong (E-RD30).

References

[1] J.F. Wang, J.P. Zhang, B.Y. Asoo, G.D. Stucky, J. Am. Chem. Soc. 125 (2003) 13966–13967.
[2] D. Wang, F. Qian, C. Yang, Z.H. Zhong, C.M. Lieber, Nano Lett. 4 (2004) 871–874.
[3] R. Beckman, E.J. Halperin, Y. Luo, J.E. Green, J.R. Heath, Science 310 (2005) 465–468.
[4] Z. Yang, Y. Huang, B. Dong, H.L. Li, Appl. Phys. A: Mater. Sci. Process. 81 (2005) 453–457.
[5] Z. Yang, Y. Huang, B. Dong, H.L. Li, J. Solid State Chem. 178 (2005) 1157–1164.
[6] H. Koizumi, N. Niizeki, T. Ikeda, Jpn. J. Appl. Phys. 3 (1964) 495–496.
[7] E. Kostiner, G.L. Shoemaker, J. Solid State Chem. 3 (1971) 186–189.
[8] D. Groult, M. Hervieu, N. Nguyen, B. Raveau, J. Solid State Chem. 76 (1988) 248–259.
[9] D. Groult, M. Hervieu, N. Nguyen, B. Raveau, J. Solid State Chem. 76 (1988) 260–265.
[10] A.S. Poghossian, H.V. Abovian, P.B. Avakian, S.H. Mkrtchian, V.M. Haroutunian, Sens. Actuators B 4 (1991) 545–549.
[11] N.I. Zakharchenko, Russ. J. Appl. Chem. 73 (2000) 2047–2051.
[12] N.I. Zakharchenko, Kinet. Catal. 43 (2002) 95–98.
[13] Y. Xiong, M.Z. Wu, Z.M. Peng, N. Jiang, Q.W. Chen, Chem. Lett. 33 (2004) 502–503.
[14] T.J. Park, G.C. Papaefthymiou, A.R. Moodenbaugh, Y.B. Mao, S.S. Wong, J. Mater. Chem. 15 (2005) 2099–2105.
[15] W.P. Lim, Z. Zhang, H.Y. Low, W.S. Chin, Angew. Chem. Int. Ed. 43 (2004) 5685–5689.
[16] S.K. Hwang, J. Lee, S.H. Jeong, P.S. Lee, K.H. Lee, Nanotechnology 16 (2005) 850–858.
[17] Y.Y. Wu, T. Livneh, Y.X. Zhang, G.S. Cheng, J.F. Wang, J. Tang, M. Moskovits, G.D. Stucky, Nano Lett. 4 (2004) 2337–2342.
[18] L.F. Cheng, X.T. Zhang, B. Liu, H.Z. Wang, Y.C. Li, Y.B. Huang, Z.L. Du, Nanotechnology 16 (2005) 1341–1345.
[19] D.H. Qin, L. Cao, Q.Y. Sun, Y. Huang, H.L. Li, Chem. Phys. Lett. 358 (2002) 484–488.
[20] C.A. Huber, T.E. Huber, M. Sadoqi, J.A. Lubin, S. Manalis, C.B. Prater, Science 263 (1994) 800–802.
[21] M. Steinhart, S. Zimmermann, P. Goring, A.K. Schaper, U. Gosele, C. Weder, J.H. Wendorff, Nano Lett. 5 (2005) 429–434.
[22] S.L. Pan, H.L. Zhang, Y. Peng, Z. Wang, H.L. Li, Chem. J. Chin. Univ. 20 (1999) 1622–1624.
[23] Y. Peng, H.L. Zhang, S.L. Pan, H.L. Li, J. Appl. Phys. 87 (2000) 7405–7408.
[24] B.B. Lakshmi, C.J. Patrissi, C.R. Martin, Chem. Mater. 9 (1997) 2544–2550.